Desmosomes: interconnected calcium-dependent structures of remarkable stability with significant integral membrane protein turnover

Reinhard Windoffer, Monika Borchert-Stuhlträger and Rudolf E. Leube*

Department of Anatomy, Johannes Gutenberg-University Mainz, Becherweg 13, 55128 Mainz, Germany
*Author for correspondence (e-mail: leube@mail.uni-mainz.de)

Accepted 23 January 2002
Journal of Cell Science 115, 1717-1732 (2002) © The Company of Biologists Ltd

Summary

Desmosomes are prominent cell adhesion structures that are major stabilizing elements, together with the attached cytoskeletal intermediate filament network, of the cytokeratin type in epithelial tissues. To examine desmosome dynamics in tightly coupled cells and in situations of decreased adhesion, fluorescent desmosomal cadherin desmocollin 2a (Dsc2a) chimeras were stably expressed in human hepatocellular carcinoma-derived PLC cells (clone PDc-13) and in Madin-Darby canine kidney cells (clone MDc-2) for the continuous monitoring of desmosomes in living cells. The hybrid polypeptides integrated specifically and without disturbance into normal-appearing desmosomes that occurred in association with typical cytokeratin filament bundles. Tracking of labeled adhesion sites throughout the cell cycle by time-lapse fluorescence microscopy revealed that they were immobile and that they maintained their structural integrity for long periods of time. Time-space diagrams further showed that desmosomal positioning was tightly controlled, even during pronounced cell shape changes, although the desmosomal arrays extended and contracted, suggesting that they were interconnected by a flexible system with intrinsic elasticity. Double-fluorescence microscopy detecting Dsc2a chimeras together with fluorescent cytokeratin 18 chimeras revealed the association and synchronous movement of labeled desmosomes and fluorescent cytokeratin filaments. Only a minor destabilization of desmosomes was observed during mitosis, demonstrated by increased diffuse plasma membrane fluorescence and the fusion of desmosomes into larger structures. Desmosomes did not disappear completely at any time in any cell, and residual cytokeratin filaments remained in association with adhesion sites throughout cell division. On the other hand, a rapid loss of desmosomes was observed upon calcium depletion, with irreversible uptake of some desmosomal particles. Simultaneously, diffusely distributed desmosomal cadherins were detected in the plasma membrane that retained the competence to nucleate the reformation of desmosomes after the cells were returned to a standard calcium-containing medium. To examine the molecular stability of desmosomes, exchange rates of fluorescent chimeras were determined by fluorescence recovery after photobleaching, thereby identifying considerable Dsc2a turnover with different rates of fluorescence recovery for PDc-13 cells (36±17% recovery after 30 minutes) and MDc-2 cells (60±20% recovery after 30 minutes). Taken together, our observations suggest that desmosomes are pliable structures capable of fine adjustment to functional demands despite their overall structural stability and relative immobility.

Movies available on-line

Key words: Cell contact, Desmosome, Intermediate filament, Live cell imaging, Green fluorescent protein, Fluorescence recovery after photobleaching

Introduction

Cell-cell adhesion is mediated by various families of plasma membrane proteins. These proteins assemble into ultrastructurally defined entities upon the stabilization of cell contacts and recruit cytoplasmic polypeptides, which in turn interact with the cortical cytoskeleton. As the dynamic maintenance of these structures is essential for tissue homeostasis, it is of general interest to understand the regulation of the various cell contacts in relationship to physiological requirements and disease. Time-lapse microscopy of living cells expressing fluorescently labeled polypeptides has opened a new avenue for examining aspects of dynamic cell-cell junction behavior. This method has revealed, for instance, that the stable-appearing cell contacts of the gap junction type change their shape, size and distribution continuously and rapidly (Jordan et al., 1999; Holm et al., 1999; Windoffer et al., 2000) and that adherens junctions are subject to considerable modulation during development (Oda and Tsukita, 1999).

In the current study, we have examined desmosomes, which are believed to be the major stabilizing cell contact type of epithelial cells. Interference with desmosomal adhesion therefore leads to reduced tissue integrity and blister formation (for reviews, see Moll and Moll, 1998; Udey and Stanley, 1999; Kowalczyk et al., 1999). Desmosomes are morphologically well defined structures (Schmidt et al., 1994; Burdett, 1998;

Kowalczyk et al., 1999) that are built around a 20-30 nm intercellular space that contains the desmoglea and is bisected by a dense midline. The cytoplasmic surfaces of both adjacent cells are decorated by electron-dense plaques that serve as anchorage sites for the intermediate filament (IF) cytoskeleton. Major desmosomal components have been identified, and their molecular interactions and topologies have been determined (for reviews, see Schmidt et al., 1994; Troyanovsky and Leube, 1998; Burdett, 1998; Kowalczyk et al., 1999; North et al., 1999). In the emerging picture, desmosomal cadherins of the desmoglein (Dsg) and desmocollin (Dsc) type take a central role by interacting laterally and transcellularly with each other and recruiting cytoplasmic plaque proteins that facilitate IF attachment. Their adhesive function is coupled to the four extracellular domains that bind to calcium and contact each other in a calcium-dependent fashion. Despite the high degree of overall divergence of their cytoplasmic domains, the three Dsg isoforms and splice variants 'a' of all three Dsc isoforms contain a region that binds to the universal plaque protein plakoglobin. In turn, the desmosomal cadherin-plakoglobin complex interacts with the desmosome-specific plaque protein desmoplakin, which also contains binding sites for the epithelial IF proteins of the cytokeratin (CK) type. Further desmosomal components, such as the plakophilins, probably modulate this basic architecture in specific but as yet poorly understood ways.

Given the stabilizing properties of desmosomes, mechanisms must exist to alter these properties during situations when rearrangements of cell-cell contact occur, for example, during mitosis and migration. To examine such changes, the modulation of calcium concentration has been used to induce rapid alterations in desmosomal adhesion in vitro. Thus, substitution of standard calcium medium (SCM) by low calcium medium (LCM) leads to the rapid loss of desmosomal adhesion by the splitting of desmosomes and endocytosis of the resulting desmosomal halves (Kartenbeck et al., 1982; Mattey and Garrod, 1986; Kartenbeck et al., 1991). In LCM, desmosomal components continue to be synthesized but are only assembled into half desmosomes (Duden and Franke, 1988; Burdett, 1993; Demlehner et al., 1995). Conversely, desmosomal adhesion is established when cells are transferred from LCM to SCM (Hennings and Holbrook, 1983; Watt et al., 1984).

Dynamic aspects of desmosomal behavior could not be directly visualized with previous methods. Even in instances of considerable desmosome reorganization, the precise sequence of events had to be painstakingly reconstructed from series of observations of cells that were fixed at different time points for analysis. Given the inherent variability between cells, it was therefore often difficult to decide whether different morphologies resulted from intercellular differences and differing reaction patterns or from simultaneously occurring stages of the same dynamic process. For example, it was not clear whether endocytosis alone accounted for the loss of desmosomal adhesion in LCM or whether and to what extent other mechanisms such as the dispersion of desmosomal components in the plasma membrane and cytoplasm contributed to this process. Similarly, it was not easy to determine whether and to what extent newly formed desmosomes were derived from preassembled half-desmosomes or from non-particulate precursors. Furthermore, nothing was known about the dynamic aspects of desmosomes in tightly coupled cells during the steady state.

As a first step to address such questions and to examine desmosomes in vivo, we have prepared cells expressing fluorescent desmosomal cadherins that are integrated into normal-appearing desmosomes. We show that these desmosomes are extremely stable and highly immobile structures that are maintained as distinct entities throughout the cell cycle together with adhering CK filaments (CKFs). On the other hand, in accordance with the above-mentioned studies, desmosomal adhesion is rapidly lost upon the reduction of calcium, leading to destabilization of desmosomes and endocytosis of desmosomal particles. Finally, we have found that, despite the extreme structural stability of desmosomes, desmosomal cadherins are rapidly exchanged.

Materials and Methods

DNA cloning

cDNA clone hDsc2.gk9 coding for human Dsc2a was generously provided by S. Schäfer and W. W. Franke (German Cancer Research Center, Heidelberg, Germany). This Bluescript-derived plasmid clone contains the entire cDNA insert of a phage clone isolated from human epidermal cDNA library HL1112b (Clontech Laboratories, Palo Alto, CA). Its insert encompasses the region between positions 8 and 3214 of the cDNA sequence denoted as DGIII by Parker et al. (Parker et al., 1991) but lacks a short fragment between positions 2549 and 2594. The 2.6 kb *Eco*RI/*Asp*I 5′ fragment of hDsc2-gk9 was subcloned together with a 156 bp polymerase chain reaction (PCR)-amplified and *Asp*I/*Bam*HI-cleaved 3′ fragment (amplimers 037 5′-GCC CAA GAC TAT GTC CTG ACA-3′; 038 5′-AAA GGA TCC TCT CTT CAT GCA TGC TTC TGC-3′) into the *Eco*RI/*Bam*HI sites of pEGFP-N1 (Clontech Laboratories), thereby generating clone C-Dsc2a.GFP-1. Expression of the green fluorescent Dsc2a chimera Dsc2a.GFP is driven by the CMV promoter in this neomycin-resistance-conferring vector. To construct cDNA clone C-Dsc2a.YFP-1 coding for yellow fluorescing Dsc2a chimera Dsc2a.YFP, the 0.75 kb *Bam*HI/*Not*I EGFP-cassette was exchanged for the corresponding cassette from pEYFP-N1 (Clontech Laboratories). To allow alternative selection in co-transfection experiments, the chimeric cDNA was also inserted into the hygromycin-resistance-providing plasmid pIRES1hyg (Clontech). To this end, a 3.5 kb *Not*I/*Bgl*II fragment was excised from C-Dsc2a.YFP-1, blunt-ended, and inserted into *Bst*XI/*Bam*HI-digested and blunt-ended pIRES1hyg (clone C-Dsc2a.YFP-2).

To prepare a cDNA construct coding for a fluorescent CK18 chimera, a 270 bp fragment of the 3′ end of the coding region of cDNA clone pHK18-P-7 (Bader et al., 1991) was first amplified by PCR with amplimers 99-16 5′- CTC AAC GGG ATC CTG CTG CA- 3′ and 99-17 5′-TTT GGT ACC CCA TGC CTC AGA ACT TTG GTG T-3′. This fragment was cloned after restriction with *Bam*HI and *Asp*718 into pBluescript KS+ (Stratagene, La Jolla, CA), and the insert was complemented by the 1 kb *Bam*HI 5′ fragment of pHK18-P-7, thereby generating clone pHK18Δstop. The complete cDNA insert of pHK18Δstop was then transferred as a *Eco*RI/*Asp*718 fragment into pECFP-N1 (Clontech Laboratories), producing clone C-HK18-CFP1, which codes for cyan fluorescent hybrid HK18.CFP whose expression is under the control of the CMV promoter and which also confers neomycin resistance.

Cell culture methods

Human hepatocellular carcinoma-derived PLC cells (ATCC CRL8024) and Madin-Darby canine kidney (MDCK) cells (clone 20; ATCC CCL-34) were passaged in DMEM (PAA Laboratories, Cölbe, Germany) supplemented with 10% fetal calf serum (Invitrogen,

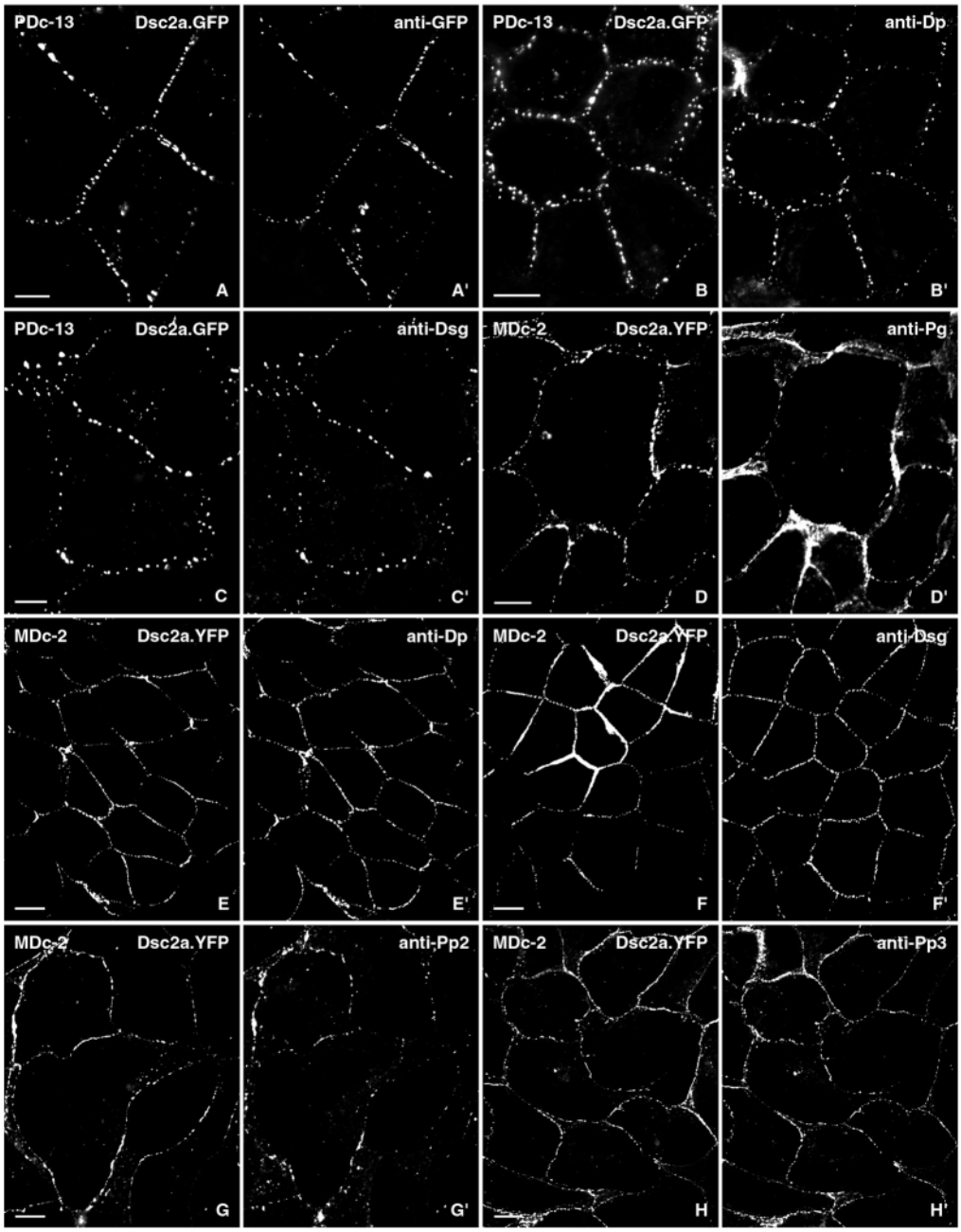

Fig. 1. Epifluorescence microscopy of cell lines stably expressing fluorescent human Dsc2a chimeras. Clone PDc-13 (A-C′) was obtained after transfection of human hepatocellular carcinoma-derived PLC cells with construct C-Dsc2a.GFP-1 coding for fusion protein Dsc2a.GFP and selection with neomycin. Clone MDc-2 (D-H′) was generated from canine kidney-derived MDCK cells by transfection with construct C-Dsc2a.YFP-2 coding for chimera Dsc2a.YFP and selection with hygromycin. The fluorescence elicited by the transgenic fusion proteins in methanol/acetone-fixed cells is shown in the micrographs on the left (A-H) and compared with the indirect immunofluorescence obtained after reaction with primary antibodies against GFP (anti-GFP), desmoplakin (anti-Dp), desmoglein (anti-Dsg), plakoglobin (anti-Pg), plakophilin 2 (anti-Pp2) and plakophilin 3 (anti-Pp3). Note the similar punctate fluorescence pattern in each picture pair, except for plakoglobin, which is detected in additional plasma membrane domains. Bars, 10 μm.

Karlsruhe, Germany). DNA constructs were introduced into these cell lines by using the calcium phosphate precipitation method (Leube, 1995). To isolate stably transfected clonal cell lines, transgenic cells were selected with either geneticin (1 mg/ml; Life Technologies, Karlsruhe, Germany) or hygromycin (150 μg/ml hygromycin; Sigma, St. Louis, MO), depending on the construct used.

In some experiments calcium concentration was reduced by using calcium-free DMEM (Invitrogen) together with fetal calf serum whose calcium concentration had been reduced to 4.6 mg/l by treatment with the anion exchanger Diaion CR11 (Supelco, Bellefonte, PA).

Immunofluorescence microscopy

Rabbit polyclonal antibodies that were raised against green fluorescent protein (GFP) and that were also reactive with the yellow and cyan fluorescent proteins (YFP and CFP, respectively) were from Molecular Probes (Eugene, OR). Murine monoclonal antibodies against desmoplakin (DP 2.15/2.17/2.20), Dsg (DG 3.10), plakophilin 2 (PP2/86) and plakophilin 3 (PKP3-270.6.2) were from Progen (Heidelberg, Germany). Monoclonal antibody 11E4 was used for the detection of plakoglobin (Kowalczyk et al., 1994). Cy3-conjugated secondary antibodies were from Biotrend (Cologne, Germany).

Electron microscopy

Electron microscopy and silver-enhanced immunoelectron microscopy with polyclonal GFP antibodies were carried out as previously described (Windoffer and Leube, 1999; Windoffer et al., 2000).

Immunoblotting and immunoprecipitation

Confluent cells were rinsed twice with ice-cold phosphate-buffered

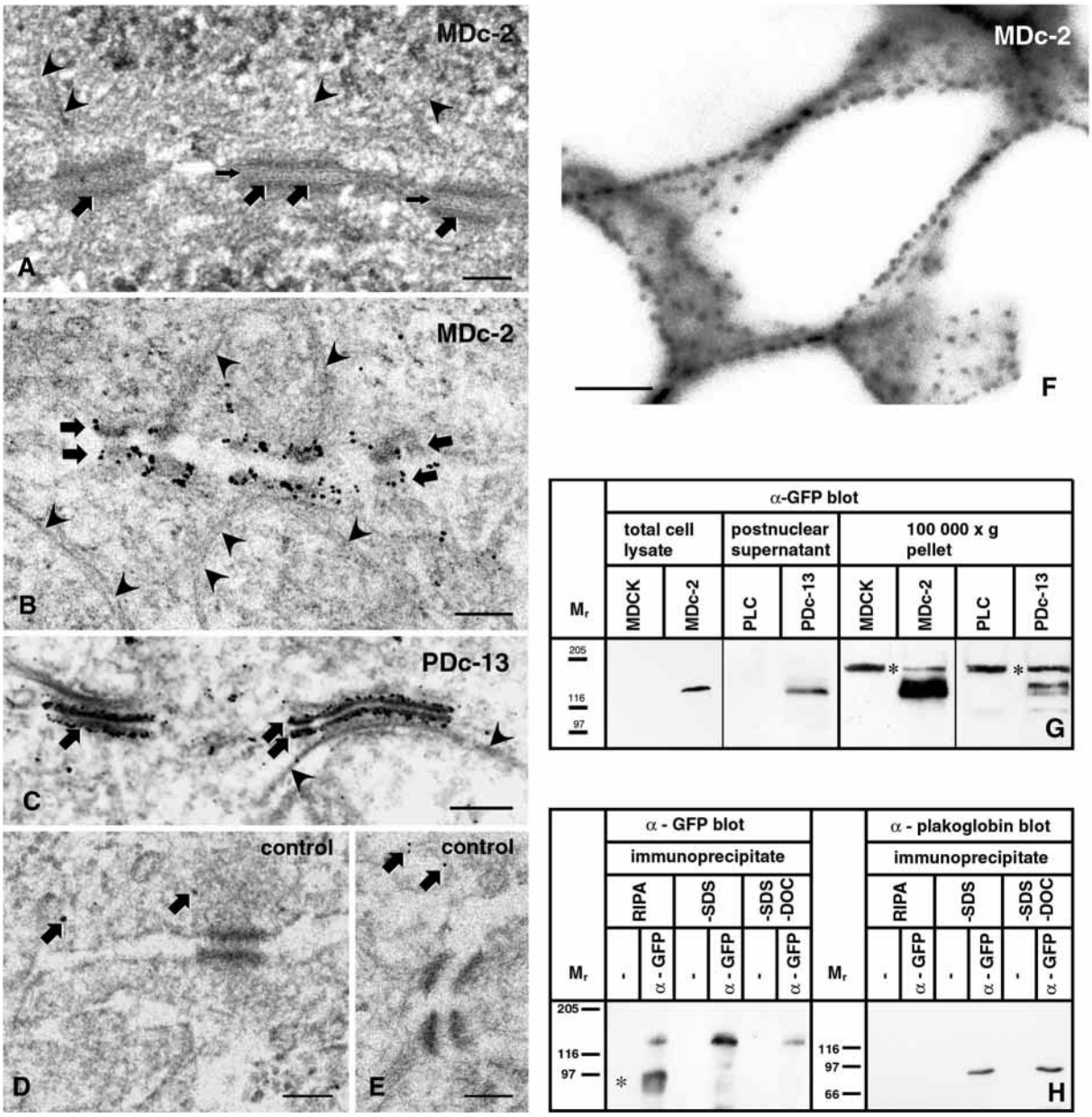

Fig. 2. Characterization of cell lines MDc-2 and PDc-13 stably expressing fluorescent Dsc2a chimeras. (A) Electron microscopy of MDc-2 cells demonstrating the normal ultrastructural appearance of desmosomes with a desmoglea-filled intercellular gap (small arrows) and symmetrical cytoplasmic plaque regions (large arrows) together with inserting IF bundles (arrowheads). Bar, 100 nm. (B-E) Immunoelectron microscopy showing abundant immunogold labelling (silver amplification) for GFP epitopes throughout the desmosomal plaque regions in MDc-2 cells (B) and PDc-13 cells (C). Arrowheads, IF bundles; arrows, desmosomal plaques. Controls are shown in D (GFP-negative cells) and E (no primary antibodies). Arrows demarcate cytoplasmic background label. Bars, 150 nm in B, 100 nm in C-E. (F) 3D reconstruction from epifluorescence micrographs that were recorded as a z-stack of eight consecutive focal planes: demonstration of the spatial dimensions of desmosomes and their arrangement in methanol/acetone-fixed MDc-2 cells. The reconstruction is also provided as movie (Movie 1; jcs.biologists.org/supplemental). Bar, 5 μm. (G) Immunoblot of 50 μg polypeptides that were derived from total cell lysates, postnuclear supernatants and 100,000 ***g*** pellets and separated by 8% SDS-PAGE. Detection of both the green and yellow fluorescent Dsc2a fusion proteins with polyclonal GFP antibodies (anti-GFP) in cDNA-transfected PDc-13 and MDc-2 cells but not in wild-type PLC and MDCK cells. The positions of coelectrophoresed molecular weight markers are shown on the left, and the relative molecular mass (M_r) is given in units of 1,000. *Position of endogenous protein crossreacting with the GFP antibodies. (H) Immunoblots of immunoprecipitates obtained from MDc-2 cells that had been lysed either in standard immunoprecipitation buffer (RIPA) or in immunoprecipitation buffer lacking SDS (–SDS) or in immunoprecipitation buffer without SDS and deoxycholate (–SDS, –DOC). For precipitation, antibodies against GFP were used that were omitted in the negative controls. The precipitates were probed either with antibodies against GFP to detect chimera Dsc2a.YFP or with antibodies against the desmosomal plaque protein plakoglobin. Note that plakoglobin is specifically coprecipitated with the chimera when the immunoprecipitation buffers lack SDS. The same molecular weight standards were used as in (G). *Position of Dsc2a.YFP degradation product.

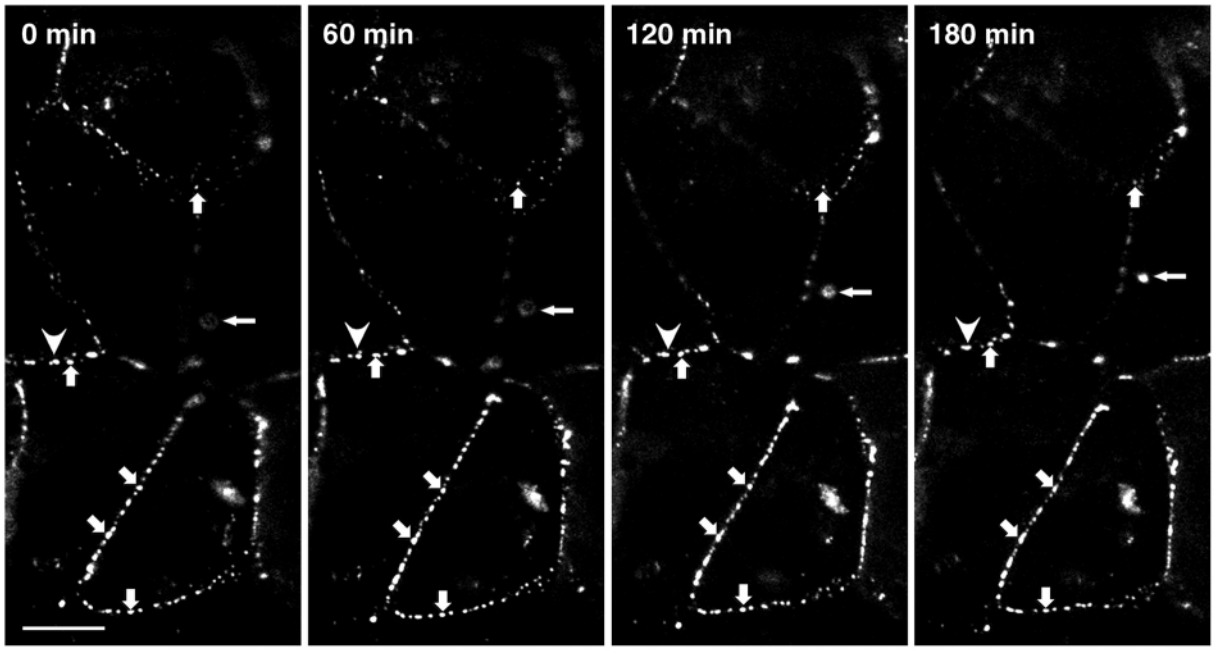

Fig. 3. Time-lapse recording of epifluorescence in PDc-13 cells expressing fluorescent Dsc2a chimera Dsc2a.GFP. Pictures were taken every 2 minutes for 3 hours and are shown in Movie 2 (jcs.biologist.org/supplemental). Large arrows demarcate desmosomes that remained in place for the entire observation period with little changes in shape and fluorescence intensity. A slowly rotating vacuolar structure in the cytoplasm is denoted by a small arrow; a rare fusion event of desmosomes is demarcated by an arrowhead. Bar, 5 μm.

saline. After removal of all fluid, cells were lysed in hypotonic H-buffer containing 10 mM Tris-HCl (pH 7.4), 1 mM EGTA, 1 mM EDTA, 2 mM dithiothreitole (DTT), 0.1 mg/ml phenylmethane sulfonylfluoride (PMSF) and 0.2 mg/ml 4-(2-aminoethyl)-benzenesulfonyl fluoride (Sigma) at 4°C. The total cell lysate was homogenized in a tight-fitting Dounce homogenizer by 30 up and down strokes. Postnuclear supernatant was then prepared by centrifugation at 1000 ***g*** for 10 minutes at 4°C. Further centrifugation of this supernatant (100,000 ***g*** at 4°C for 1 hour) yielded a 100,000 ***g*** pellet fraction that was dissolved in H-buffer. Total cell lysates, postnuclear supernatant fractions, and the 100,000 ***g*** fractions were diluted 1:1 in loading buffer (2% (w/v) SDS, 150 mM DTT, 0.005% (w/v) bromophenol blue, 30 mM Tris-HCl pH 6.8, 10% (w/v) glycerol) and subjected to SDS polyacrylamide gel electrophoresis (SDS-PAGE), electroblot transfer and antibody incubation (Windoffer and Leube, 1999; Windoffer et al., 2000). Detection of bound horseradish-peroxidase-coupled secondary antibodies was performed with the help of enhanced chemiluminescence (Amersham Pharmacia Biotech, Freiburg, Germany).

For immunoprecipitation experiments, confluent cells were washed twice in phosphate-buffered saline at 4°C. After complete removal of all fluid, 3.5 ml immunoprecipitation buffer was added per 10 cm diameter Petri dish. Three different immunoprecipitation buffers were used: (1) RIPA buffer (10 mM Na_2HPO_4 (pH 7.2), 150 mM NaCl, 2 mM EDTA, 1% (v/v) Triton X-100, 0.25% (w/v) SDS, 1% (w/v) sodium deoxycholate, 2 mM PMSF), (2) RIPA buffer without SDS or (3) RIPA buffer without SDS and sodium deoxycholate. Cells were incubated in the respective buffer for 30 minutes at 4°C with

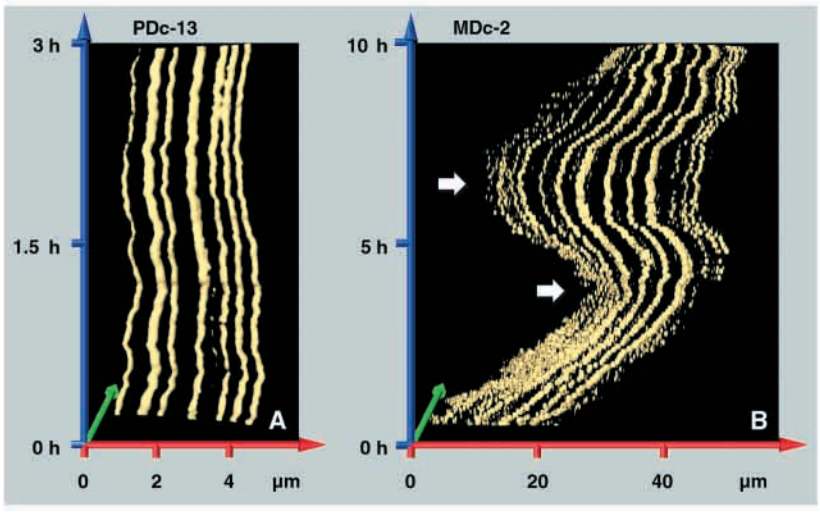

Fig. 4. Time-space diagrams depicting coordinated desmosome-motility in PDc-13 cells (A) and MDc-2 cells (B) stably expressing fluorescent Dsc2a chimeras. The diagram on the left was derived from a time-lapse fluorescence recording of a cell contact region that was imaged for 3 hours at 2 minute intervals (Movie 3; jcs.biologists.org/supplemental); the diagram at right was derived from a time-lapse fluorescence recording of a desmosomal array that was monitored for 10 hours at 5 minute intervals (Movie 4). Time is plotted along the y-axis in hours (h), whereas movement in the 2D space dimensions is plotted along the x- and z-axis in μm. The rough and sometimes interrupted surface of the desmosomal trajectories in MDc-2 cells is the result of the comparatively long recording intervals. Note the coordinated movement, constant arrangement, size and shape of the depicted desmosomes, whereas interdesmosomal distance varies considerably, albeit in a coordinated fashion (compare, for example, time points marked by arrows).

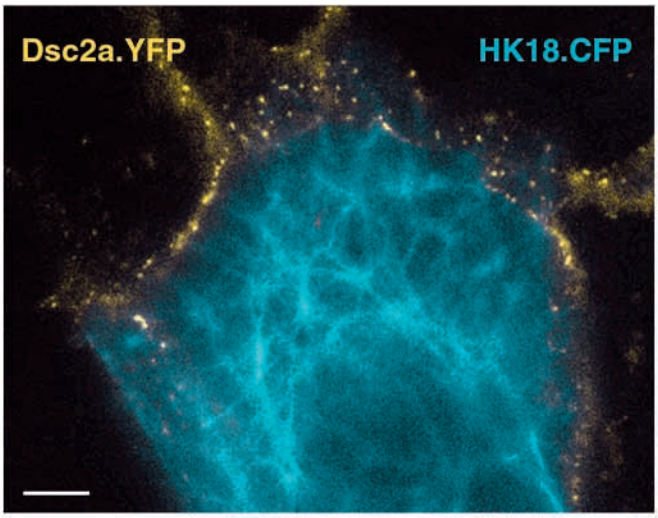

Fig. 5. Double-epifluorescence microscopy of living MDc-2 cells stably expressing Dsc2a chimera Dsc2a.YFP, including a transiently transfected cell synthesizing, in addition, fluorescent CK 18 chimera HK18-CFP. The picture shown is taken from a time-lapse recording (Movie 5; jcs.biologists.org/supplemental). Fluorescence is depicted in false colors in the movie for better visualization, denoting Dsc2a.YFP-containing desmosomes in red and HK18-CFP-positive CKFs in green. All micrographs of the movie and the picture shown in the figure consist of five superimposed focal recordings that were taken at each time point after excitation at 498 nm (YFP) and 436 nm (CFP). Bar, 5 μm.

occasional shaking and then scraped off. Homogenization was carried out with a tight-fitting Dounce homogenizer by 30 up and down strokes. Lysed material was cleared by centrifugation at 40,000 ***g*** for 50 minutes at 4°C, and the supernatant was incubated with anti-GFP antibodies (see above) overnight at 4°C on an overhead roller. As a negative control, the homogenate was incubated in parallel without the antibody. To each sample, 15-20 mg pre-swollen protein-A-sepharose (type CL-4B; Amersham Pharmacia Biotech, Freiburg, Germany) was added per milliliter immunoprecipitation buffer followed by an incubation for 1-2 hours at 4°C. Subsequently, the sepharose was spun down at 2000 ***g*** in a table-top centrifuge for 10 minutes at 4°C, followed by three wash cycles in buffer containing 0.5% (w/v) Tween-20, 50 mM Tris-HCl pH 7.5, 150 mM NaCl and 0.1 mM EDTA, and five wash cycles in buffer containing 0.5% (w/v) Tween-20, 100 mM Tris-HCl pH 7.5, 200 mM NaCl and 2 M urea. Finally, the sepharose was washed in phosphate-buffered saline supplemented with 1% (w/v) Triton X-100 and then dissolved directly in loading buffer. After being boiled for 5 minutes and a brief centrifugation step, the supernatants were loaded on 8% SDS-polyacrylamide gels for electrophoresis and immunoblotting with either anti-GFP antibodies (dilution 1:1,000) or anti-plakoglobin antibodies 11E4 (dilution 1:70). Bound antibodies were detected with an enhanced chemiluminescence system.

Live cell imaging

The culture chamber and culture conditions used for time-lapse fluorescence microscopy of living cells have previously been described in detail (Windoffer and Leube, 1999; Windoffer et al., 2000). Images were recorded in some instances with a confocal laser scan microscope (Leica TCS NT, Leica Microsystems, Wetzlar, Germany) as described (Windoffer and Leube, 2001) and, in most instances, by epifluorescence microscopy with either of the recording devices described previously (Windoffer and Leube, 1999; Windoffer et al., 2000) or an imaging system with inverse optics from Olympus (Hamburg, Germany). The latter system was equipped with a monochromator for excitation and a piezo-driven z-axis stepper attached to the 60× 1.4 N.A. oil immersion objective. Pictures were recorded with an IMAGO slow scan charged-coupled device camera, and the system was controlled by TILLvisION software. The microscope was kept in a climate chamber at 37°C with the cells either in a closed culture chamber (see above) or in a Petri dish with a glass bottom (Mattek, Ashland, MA). Excitation was at 496 nm for enhanced GFP, 498 nm for enhanced YFP and 436 nm for enhanced CFP. For a 3D delineation of structures, multiple focal planes were recorded for each time point by using the piezo stepper. The resulting picture stacks were either projected on top of each other or were used to prepare 3D reconstructions with the help of Amira (TGS) software.

Image sequences were edited with Image-Pro Plus 4.5 (Media Cybernetics) and were converted into QuickTime movies (Apple) (see jcs.biologists.org/supplemental). To edit single pictures and to arrange them into figures, Photoshop software (Adobe Photoshop 5.0) was used.

To compute time-space diagrams, rows of labeled desmosomes were cut out from recordings at each time point, and the resulting pictures were imported into Amira. The image data were compiled, producing trajectories that present the surface view of individual desmosomes in time and space.

Photobleaching experiments were carried out with a Leica TCS SP2 confocal microscope. The 488 nm line of an argon/krypton laser was used for both bleaching and image recording. The emitted light was monitored between 500 nm and 590 nm. Recordings were performed via a 63× 1.4 N.A. oil immersion objective. Standard settings for prebleach and recovery image scans were 6% of minimum laser power, a line average of 4 and a gain of 800. A wide pinhole size (setting of 500) was chosen for high depth of focus, minimal photobleaching and strong fluorescence signal. Rows of desmosomes that were straight for several micrometers were selected for bleaching to be able to define rectangular areas of interest. Bleaching in the chosen areas of interest was carried out at 100% of medium laser power for a total of 20 scans. Under these conditions, bleaching was practically complete not only in the focal recording plane but also in the regions above and below, thereby excluding the possibility that focal shift or cell motility was erroneously taken as a source for fluorescence recovery. The microscope was set to prebleach parameters immediately after bleaching, and images were recorded at intervals of 5 minutes. The recording time was limited to 30 minutes, since cell-shape changes resulted in the movement of desmosomal arrays in and out of the area of interest, thereby preventing the correct measurements of recovery at later time points. The gray values of the bleached areas were measured in the recorded 12 bit image data (Image-Pro Plus 4.5), analyzed by using spreadsheet routines (Excel) and drawn into diagrams.

To obtain optimal spatial resolution, the pinhole size was reduced (setting of 90) in some experiments. In these instances, 10 focal planes were recorded prior to bleaching, immediately after bleaching and after a 30 minute recovery period.

Results

Fluorescent Dsc2a chimeras are integrated into normal desmosomes

To examine the dynamics of desmosomes in living cells, we decided to construct hybrid cDNAs for the expression of fluorescent protein chimeras that should be targeted specifically to desmosomes. The most promising candidates for this purpose were the desmosomal cadherins, since they are essential and exclusive components of desmosomes. Furthermore, additions to their variable cytoplasmic C-termini

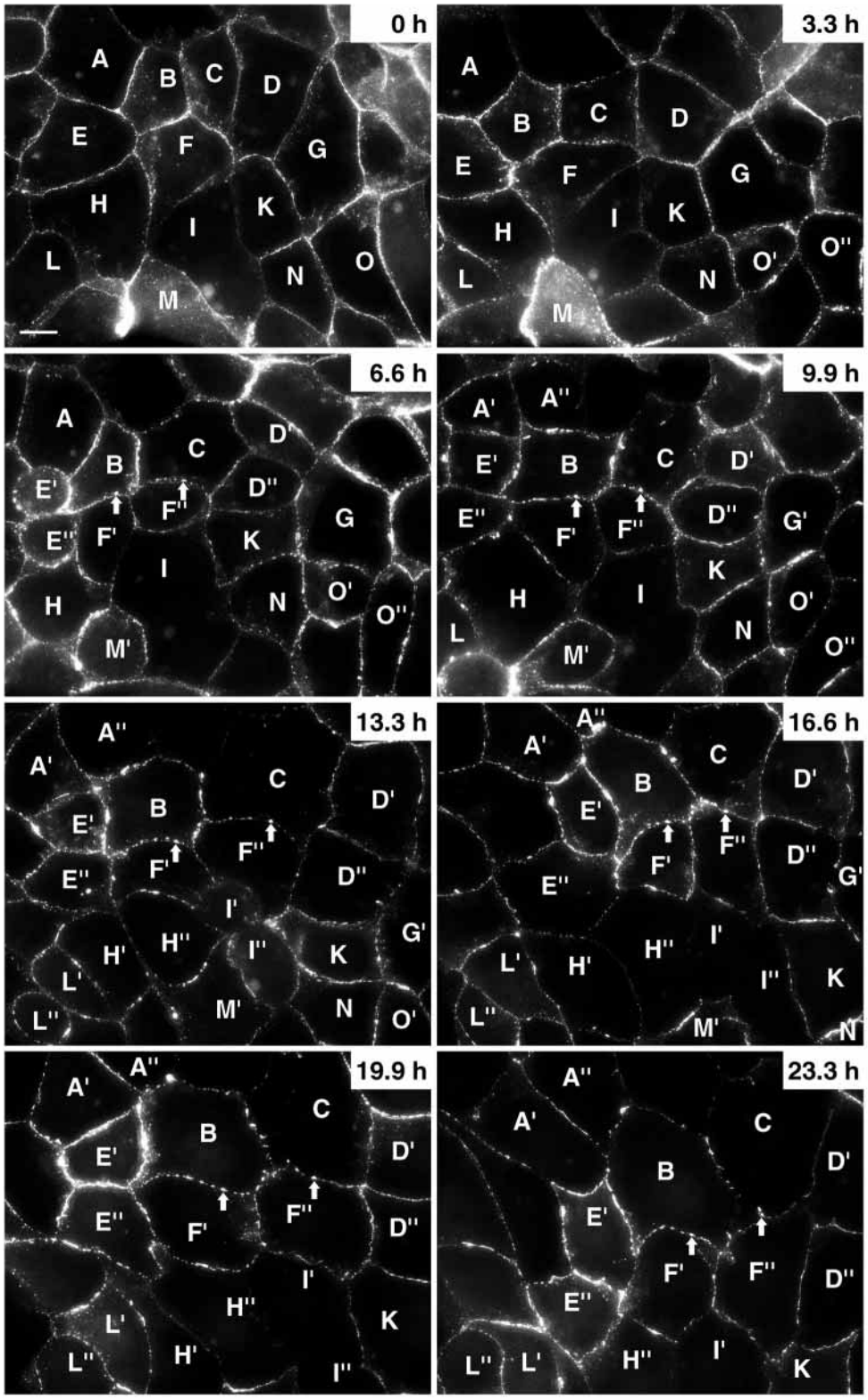

Fig. 6. Epifluorescence microscopy of live MDc-2 monolayer monitoring the distribution of fluorescent chimera Dsc2a.YFP for 23.3 hours. The pictures are taken from a time-lapse recording (Movie 6; jcs.biologists.org/supplemental), for which seven focal planes were imaged every 5 minutes. The projection images are shown. Individual cells are labeled by letters, and daughter cells that are generated during the observation period are denoted by ′ and ″. Note the maintenance of desmosomes for very long periods (arrows). Bar, 10 μm.

have been shown to be tolerated with no apparent functional defects, provided that expression levels are not too high (Norvell and Green, 1998). Therefore, cDNAs coding for different fluorescent proteins were cloned next to the 3′ end of the desmosomal cadherin Dsc2a cDNA in eukaryotic expression vectors. Transient transfections of these recombined vectors into a number of different epithelial cell lines of human origin, including hepatocellular carcinoma PLC cells, colon adenocarcinoma CaCo-2 cells, cervix-carcinoma HeLa cells and vulvar squamous cell carcinoma A-431 cells, as well as bovine mammary gland-derived MDBK cells or Mardin-Darby canine kidney MDCK cells, conferred a

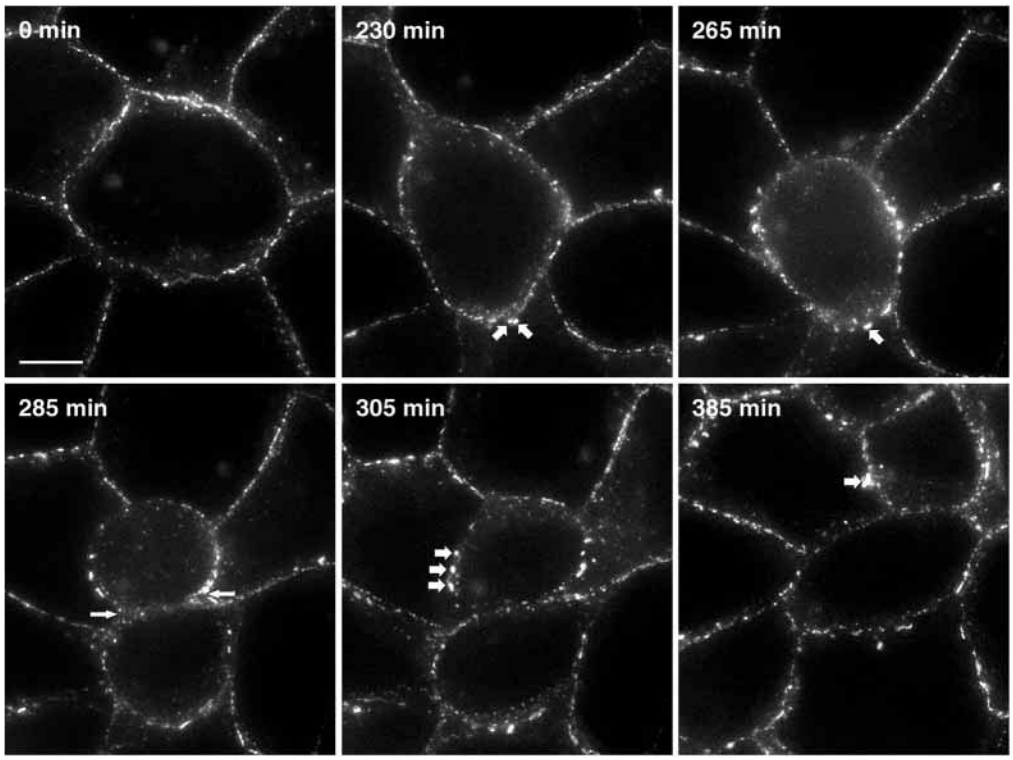

Fig. 7. Detail taken from Fig. 6 to demonstrate the characteristic stages of desmosome distribution during mitosis at higher magnification. The entire image series is provided as Movie 7 (recording intervals 5 minutes). Each picture consists of seven focal planes that were superimposed. Note the transient increase of diffuse fluorescence (265 minutes, 285 minutes), ongoing fusion of desmosomes (large arows), the enrichment of fluorescent puncta around the cleavage furrow (thin arrows in 285 min) and the continued presence of desmosomes at all time points. Bar, 5 μm.

multipunctate epifluorescence pattern that was primarily restricted to cell-cell contact regions in each case (not shown). Occasionally, polymorphic reactivity was also noted in the cytoplasm. The fluorescence pattern was indistinguishable between living and fixed cells and was independent of the promoter used.

For further analyses, stable cell clones were established from PLC and MDCK cells, two of which are described in detail in this communication. PLC subline PDc-13 was obtained after transfection with plasmid C-Dsc2a.GFP-1, driving the expression of the green fluorescent fusion protein Dsc2a.GFP with the help of the CMV promoter. The Dsc2a.GFP fluorescence pattern was almost identical to that observed by indirect immunofluorescence with antibodies against GFP (Fig. 1A,A′). Therefore, GFP fluorescence reflects the distribution of the hybrid polypeptides within the entire cell. The transgene products were almost exclusively detected in puncta at the cell surface where they were colocalized with the desmosomal plaque protein desmoplakin (Fig. 1B,B′) and Dsg2, the other desmosomal cadherin of PLC cells (Fig. 1C,C′) (Schäfer et al., 1994). MDCK-derived clone MDc-2 synthesized the yellow fluorescent Dsc2a chimera Dsc2a.YFP from plasmid C-Dsc2a.YFP-2. In this case, fluorescent puncta representing individual desmosomes were much smaller and more tightly spaced than in PDc-13 cells (Fig. 1D-H), in accordance with the desmosome staining of the corresponding wild-type cell lines by indirect immunofluorescence (not shown).

Furthermore, double fluorescence microscopy of fixed MDc-2 cells also revealed that the chimeras colocalized with the desmosomal proteins plakoglobin, desmoplakin, Dsg, plakophilin 2 and plakophilin 3 (Fig. 1D-H). As expected, antibody staining with the universal plaque protein plakoglobin displayed additional non-desmosomal plasma membrane domains (Fig. 1D,D'). All staining patterns were indistinguishable from those observed in wild-type non-transfected cells (not shown), indicating that the transgene expression did not affect desmosome formation and composition and that Dsc2a mutants were not mistargeted. In addition, the ultrastructure of desmosomes in both transgenic cell lines was indistinguishable from that of wild-type cells, presenting cytoplasmic plaques with inserting IFs, a defined intercellular space with desmoglea, and in some instances, a recognizable midline (Fig. 2A).

Immunoelectron microscopy with GFP antibodies also showed that the fusion proteins were highly enriched in typical desmosomes with an even distribution throughout the plaque regions (Fig. 2B,C; controls in Fig. 2D,E). Anchorage of CKF bundles was normal in these strongly labeled desmosomes.

To characterize further the morphology and distribution of desmosomes in the cDNA-transfected cell lines, 3D-reconstructions were produced from stacks of serial focal fluorescence images. Fig. 2F and the corresponding Movie 1 (see jcs.biologist.org/supplemental), which contains an animated version of the reconstruction, show the macular, that is, dot-like, morphology of desmosomes, which are arranged as several circumferential lines around MDc-2 cells. In addition, some diffuse non-desmosomal fluorescence was seen that was apparently located in the plasma membrane. Similar 3D reconstructions were obtained from wild-type cells in which desmosomes had been labeled by indirect immunofluorescence microscopy.

Immunoblotting of cell fractions with GFP antibodies revealed that fusion proteins of the expected size (calculated M_r of the mature polypeptide chimera is 123,381) were synthesized in both cell lines and were detectable in total cell

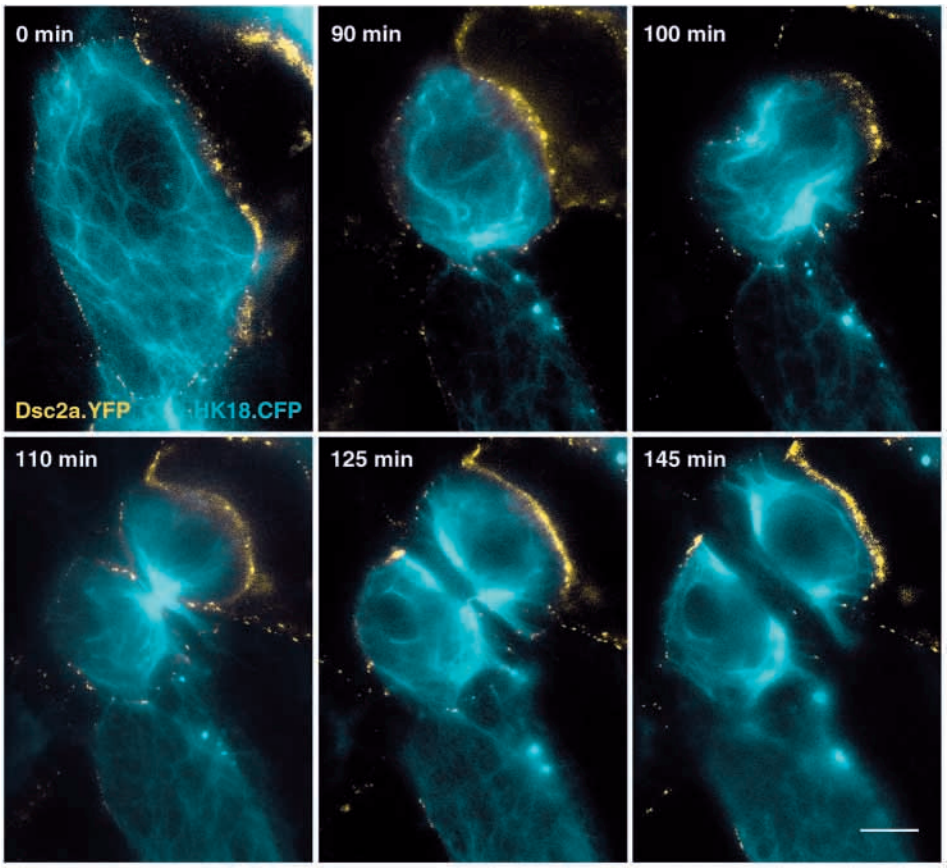

Fig. 8. Double epifluorescence microscopy of live MDc-2 cells showing the distribution of Dsc2a.YFP and HK18-CFP during mitosis. Images at each time point represent the projection of six pictures (z-distance of 0.5 μm) recording the fluorescence emitted after excitation at 498 nm (YFP chimera) and 436 nm (CFP chimera). The complete series of images is provided as Movie 8 (jcs.biologists.org/supplemental) (recording intervals 5 minutes; same color code as in Movie 5). Note the continued presence of Dsc2a.YFP-positive desmosomes throughout cell division, and the considerable alterations in the HK18-CFP-containing CKF system with some residual desmosome-associated material. Bar 5 μm.

lysates, postnuclear supernatant fractions and 100,000 ***g*** pellets (Fig. 2G). To determine whether Dsc2a chimeras interact with plakoglobin, the major desmosomal cadherin-associated plaque molecule (Troyanovsky and Leube, 1998), coimmunoprecipitation experiments were performed. These showed a specific association of both molecules in a high salt buffer containing 1% deoxycholate and 1% Triton-X-100, but this could be disrupted by SDS (Fig. 2H). Taken together, our observations demonstrate that Dsc2a chimeras are integrated into structurally and functionally competent desmosomes in PDc-13 and MDc-2 cells and that the punctate fluorescence conveyed by these molecules can therefore be used for the monitoring of desmosome dynamics in these cells.

Desmosomes are static and interconnected throughout interphase

Time-lapse fluorescence microscopy of PDc-13 and MDc-2 cells was performed to monitor desmosome behavior in vivo. A series of pictures taken from a recording of PDc-13 cells (Movie 2; jcs.biologists.org/supplemental) is shown in Fig. 3. In this sequence, individual desmosomes could be traced throughout the entire observation period of 3 hours. However, the motility of cells within the monolayer often resulted in cell-shape changes, leading to a shift of desmosomes. In general, most desmosomes maintained their particular appearance and fluorescence intensity and remained separate. Fusion and fission of desmosomes was rare (the arrowheads in Fig. 3 show fusion of small desmosomes into larger structure). Occasionally, fluorescent vacuolar structures that moved very little, except for some local gyrating motility, and that did not seem to exchange with the other fluorescent components (small arrows in Fig. 3), were detected in the cytoplasm. Similar results were also obtained in MDc-2 cells by time-lapse fluorescence microscopy (see below), although the small size and close spacing of desmosomes made it more difficult to follow them individually.

Time-space diagrams were constructed for the graphical visualization of desmosome motility. To this end, continuous shape reconstructions were prepared from a series of 2D images in time and space, the resulting trajectories depicting motilities in the x-y directions during time. A contact region of tightly associated PDc-13 cells was used for the computation of the diagram in Fig. 4A (see also Movie 3 at jcs.biologists.org/supplemental). It demonstrates that these desmosomes moved only very little during the 3 hour recording time. Furthermore, the size, shape and fluorescence intensity of individual desmosomes were maintained throughout. Interestingly, the minor movements of desmosomes appeared to be coordinated. The diagram shown for a contact region taken from a growing but confluent MDc-2 culture in Fig. 4B depicts the same phenomenon (see Movie 4 at jcs.biologists.org/supplemental). Remarkably, despite migration of the cell for over 30 μm, that is, more than the cell's diameter, the relative position of the desmosomes remained the sample for 10 hours without significant exchange or crossing over between the different time tracks. However, significant overall flexibility of the contact area was seen, which almost doubled in size at times (compare the time points marked by arrows in Fig. 4B).

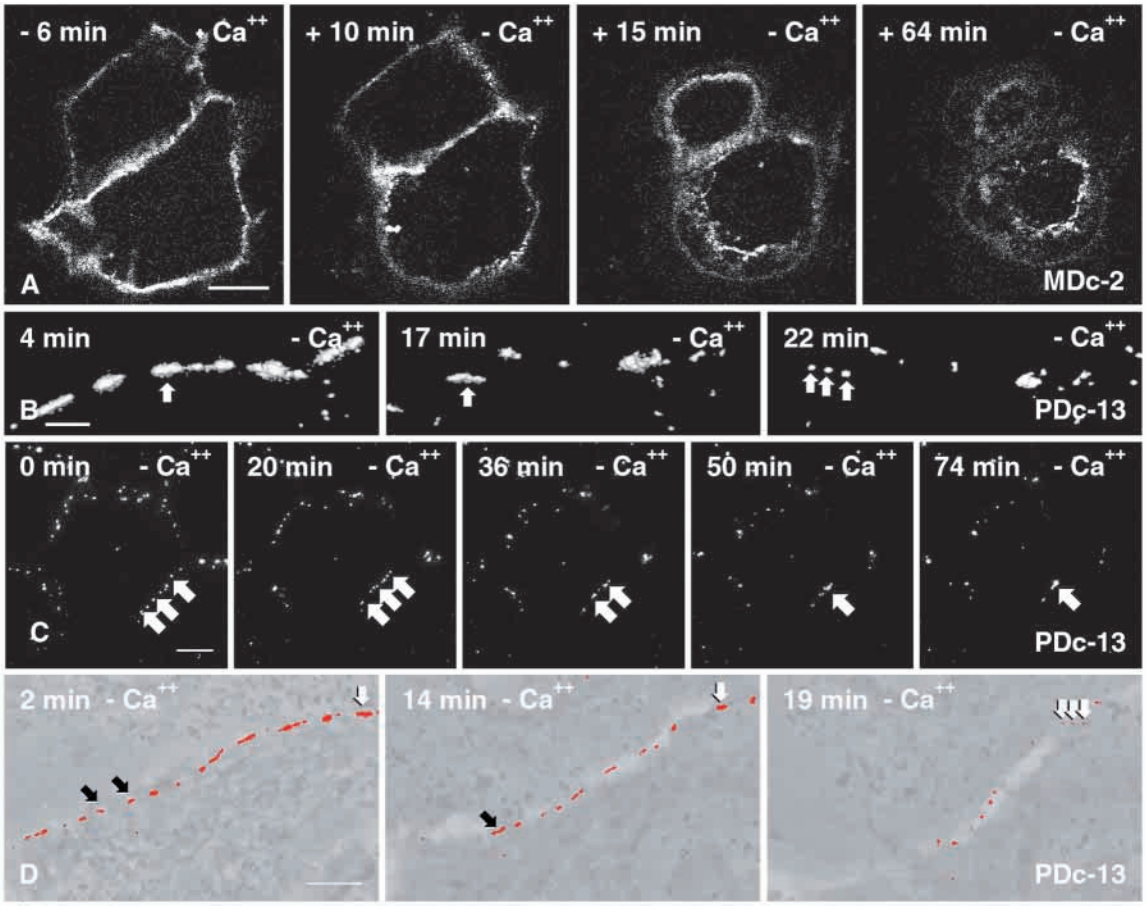

Fig. 9. Time-lapse fluorescence microscopy of cells expressing fluorescent Dsc2a chimeras depicting alterations in desmosomal cadherin distribution upon reduction of Ca^{++}. Cells were transferred from SCM (+ Ca^{++}) to LCM (– Ca^{++}) as indicated. (A) Confocal laser scan microscopy of MDc-2 cells using a large pinhole. The pictures are taken from Movie 9 (1 minute recording intervals) depicting the internalization of Dsc2a.YFP-containing desmosomal particles and the continued presence of diffuse non-desmosomal Dsc2a.YFP fluorescence at the cell surface. Bar, 10 μm. (B) 3D reconstruction of z-stacks each consisting of five epifluorescence micrographs showing the disintegration of large Dsc2a.GFP-labeled desmosomal structures into smaller particles in PDc-13 cells after the reduction of the Ca^{++} concentration (arrows). The complete sequence is provided as Movie 10 (1 minute recording intervals; jcs.biologists.org/supplemental). Bar, 5 μm. (C) Projection images of z-stacks, each consisting of five focal planes recording epifluorescence of Dsc2a.GFP in PDc-13 cells. Note the fusion of small fluorescent desmosomal particles after the reduction of Ca^{2+} (arrows). The entire image series is presented in Movie 11 (2 minute recording intervals). Bar, 5 μm. (D) Overlay of projected fluorescence pictures (5 focal planes) and corresponding phase contrast micrographs obtained from Movie 12 (jcs.biologists.org/supplemenal), which was recorded in PDc-13 cells. Note the overall reduction of desmosomes together with the fusion of desmosomes (black arrows) and fission of desmosomes (white arrows) after removal of calcium. Bar, 10 μm.

To characterize the dynamic relationship between desmosomes and the adhering CK cytoskeleton, double fluorescence time-lapse microscopy was performed in cells that coexpressed Dsc2a.YFP together with HK18.CFP, a human CK 18-ECFP chimera (see also Windoffer and Leube, 1999; Strnad et al., 2001; Windoffer and Leube, 2001). To this end, HK18.CFP was transiently expressed in MDc-2 cells by cDNA transfection of plasmid C-HK18-CFP1. An example of a doubly transfected cell demonstrating that peripheral filaments extending from the dense filamentous mesh are in close proximity to desmosomes is depicted in Fig. 5. Since multiple focal images were superimposed to generate this picture, plasma-membrane-localized desmosomes are seen in different peripheral domains of the rounded cell surface contours. The live cell imaging in Movie 5 (jcs.biologist.org/supplemental) presenting Dsc2a.YFP fluroescence in red and HK18.CFP fluorescence in green reveals that desmosome-attached CKFs move in synchrony with their respective adhesion sites (best resolved at top cell margin).

Desmosomes are maintained during the entire cell cycle but show signs of destabilization during mitosis

To characterize the dynamic aspects of desmosomes further, fluorescence emitted by the desmosomal cadherin chimeras was monitored throughout the life cycle of individual cells and their progeny. A day-long recording of a confluent MDc-2 cell culture is presented in Fig. 6 and Movie 6 (available at jcs.biologist.org). Each image presents a projection of seven focal planes. Nine cell divisions took place during this time within the observation field, resulting in major rearrangements that were accompanied by changes in cell shape and movement

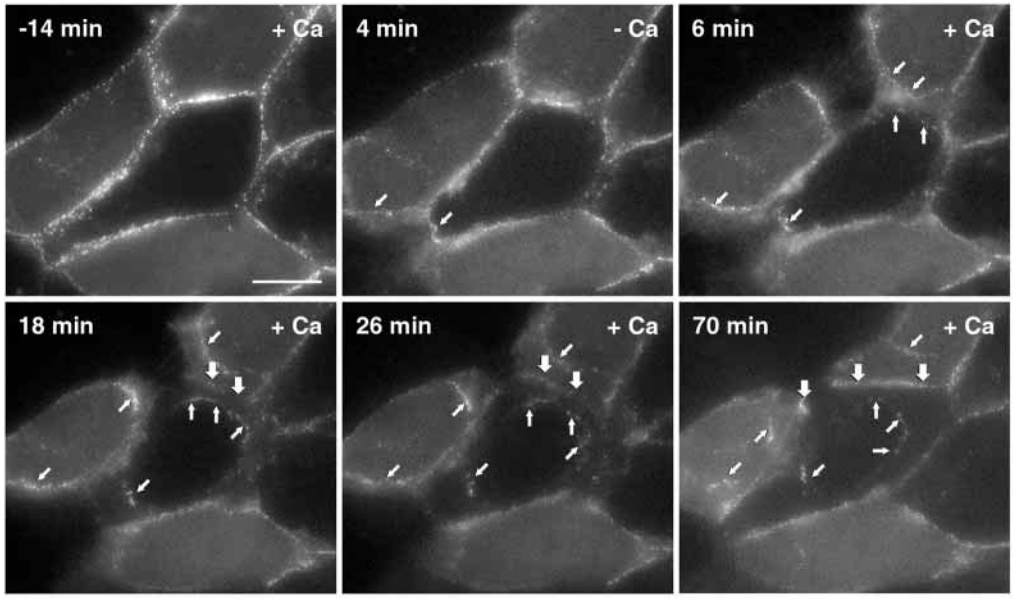

Fig. 10. Time-lapse epifluorescence microscopy of MDc-2 cells monitoring the distribution of Dsc2a.YFP in response to a transient 5 minute reduction of Ca^{2+}. The entire sequence is shown as Movie 13 (jcs.biologists.org/supplemental; 2 minute recording intervals). Note the uptake of fluorescent puncta into the cytoplasm shortly after the pulse of LCM and their continued presence in this location (small arrows), whereas small dots re-appear at the cell surface (large arrows). Bar, 10 μm.

of cells in and out of the recording area. Nevertheless, despite these pronounced dynamic processes, desmosomes were always visible as distinct entities in all cells. Furthermore, individual desmosomes could be traced for very long periods of time (two examples are labeled by arrows).

The pronounced cell-shape changes that occurred during mitosis made it difficult to follow individual desmosomes throughout cell division. However, some details that were consistently observed are demonstrated in Fig. 7 and Movie 7 (available at jcs.biologists.org), which presents projections of multiple focal recordings of a mitotic cell at high magnification (compare with Fig. 6 and Movie 6 (jcs.biologists.org/supplemental)). During prometaphase, diffuse fluorescence increased considerably, either as a consequence of the dispersion of chimeric polypeptides (compare 0 minutes with 265 minutes) and/or as a result of the altered cell shape. In addition, many desmosomes fused, thereby generating large fluorescent plaques (arrows at 230 minutes and 265 minutes). During cytokinesis, an enrichment of desmosomal fluorescence was noted around the region of the cleavage furrow (arrows at 285 minutes). After completion of cytokinesis, the diffuse fluorescence was rapidly lost and the finely punctate desmosomal fluorescence was re-established, although large plaques remained (arrow in 385 minutes). It should be stressed that we did not observe the complete loss of desmosomal cell contacts at any point during mitosis in any of our recordings.

To characterize the relative distribution and organization patterns of desmosomes and the CKF cytoskeleton during mitosis, we also performed double fluorescence microscopy of dividing MDc-2 cells that were transiently transfected with constructs coding for fluorescent CK chimeras. The mitotic CKF alterations in MDCK cells differ from those previously reported for A-431 cells (Windoffer and Leube, 1999; Windoffer and Leube, 2001) in that the CKF network is not completely disassembled into soluble subunits and granular aggregates but is, instead, compacted for the most part into densely bundled material. This material subsequently separates during cytokinesis into two parts that are distributed into the daughter cells from which new networks are formed. In MDc-2 cells expressing HK18-CFP some peripheral CKFs were identified that remained in association with desmosomes during cell division (Fig. 8) (Movie 8 at jcs.biologists.org/supplemental).

Desmosome stability is lost upon calcium reduction resulting in the irreversible uptake of desmosomal particles but retaining desmosomal cadherins with desmosome-forming capacity

In the next set of experiments, we studied the effect of calcium reduction on desmosome dynamics. MDc-2 cells started to contract within a few minutes of transfer from SCM to LCM and rounded up progressively. Fluorescent puncta were translocated into the cell interior where they formed a circumferential ring around the nucleus (Fig. 9A) (Movie 9 at jcs.biologists.org/supplemental). These puncta colocalized with desmoplakin and Dsg (not shown), suggesting that complex structures were taken up and not just individual polypeptides. Remarkably, some diffuse Dsc2a.YFP fluorescence was detected at the cell surface (+15 minutes and +64 minutes in Fig. 9A). Within a few hours, the cytoplasmic dots lost their fluorescence completely. Calcium reduction also led to the collapse of the CKF cytoskeleton and to the formation of a dense perinuclear ring of actin filaments, whereas microtubules were not visibly affected (not shown). We could further demonstrate, in wild-type MDCK cells, that endocytosis took place independently of the CKF system but required an intact actin system (not shown). Endocytosis of desmosomal fluorescence could not be induced in PDc-13 cells and was not observed in MDc-2 cells more than 3 days after plating. However, fusion of desmosomes into larger structures and, conversely, the separation into smaller particles, occurred much more frequently in these cells in LCM than in SCM (Fig. 9B-D) (Movies 10-12; available at jcs.biologists.org/supplemental), indicating that desmosome stability was also considerably compromised by calcium reduction.

An attractive implication of the calcium-switch model is the potential re-utilization of endocytosed desmosomal particles

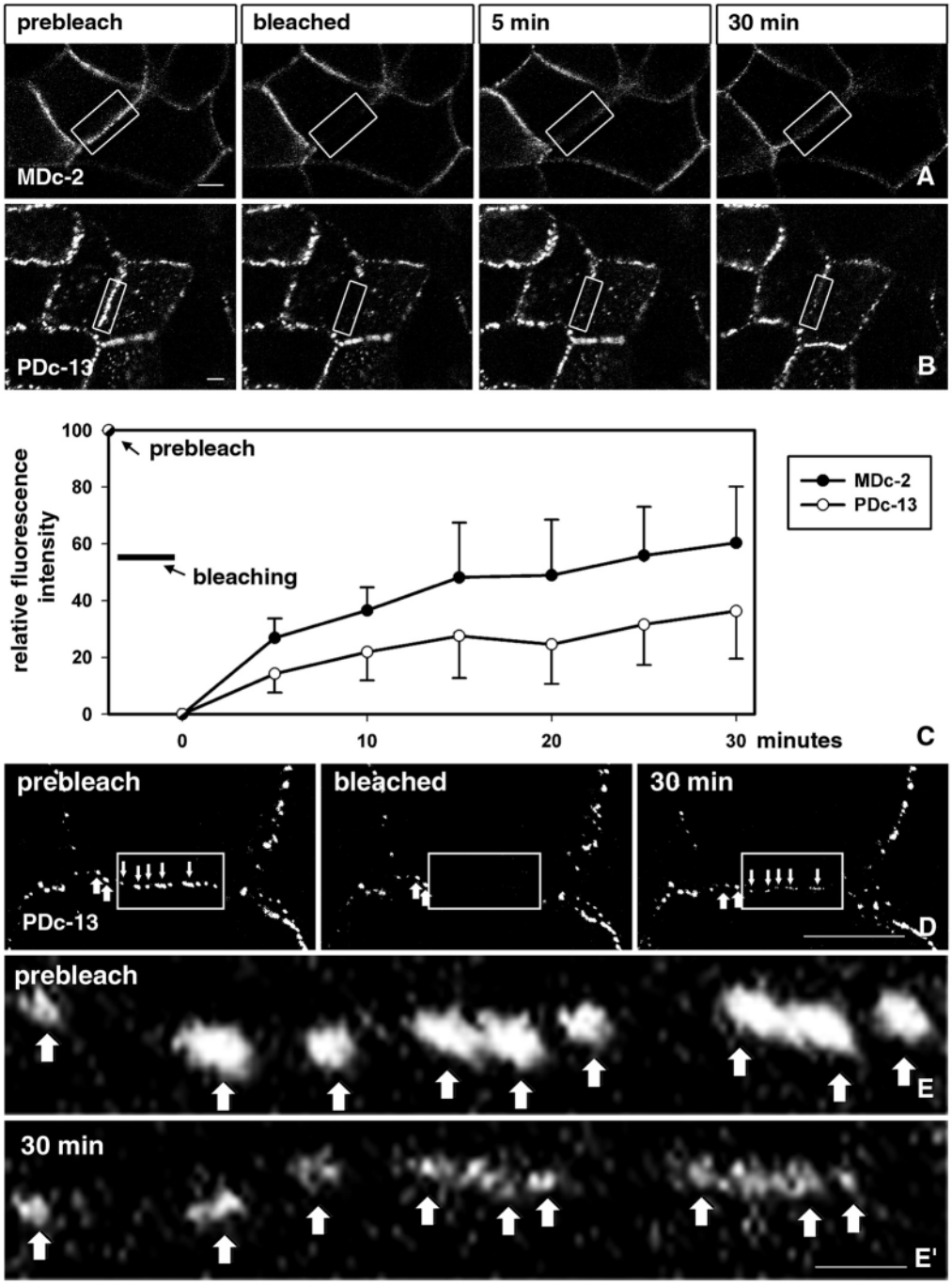

Fig. 11. FRAP analyses in MDc-2 and PDc-13 cells. A representative series of photomicrographs of single confocal sections that were recorded with a large pinhole is depicted for MDc-2 (A) and PDc-13 cells (B). The bleached areas are demarcated by boxes. Note the strong desmosomal fluorescence before bleaching (prebleach); this fluorescence is completely destroyed by bleaching (bleached) but recovers to a considerable degree within 30 minutes (5 min, 30 min). Bars, 5 μm. (C) The graphs show digital representations of pooled results from MDc-2 (*n*=6) and PDc-13 cells (*n*=10). The means of the relative fluorescence intensities are blotted as functions of time. (D) Confocal fluorescence recording of bleaching in PDc-13 cells; microscope settings were adjusted for high spatial resolution (small pinhole). E,E′ show a high magnification of the bleached area prior to bleaching and after a 30 minute recovery period. Note the re-emergence of fluorescence in desmosomal structures (arrows in D,E,E′). Bars, 10 μm in D, 1 μm in E′.

for desmosome re-formation, as has been suggested for components of other adherens junctions (Le et al., 1999; Akhtar and Hotchin, 2001). However, in accordance with earlier studies (e.g. Mattey and Garrod, 1986; Garrod et al., 1990), we did not observe the retranslocation of endocytosed structures to the cell surface after cells were returned to normal calcium-containing medium. We speculated that the uptake of desmosomal particles deep into the cell interior may be irreversible, whereas this may not be the case at earlier stages. Therefore, the calcium level was only reduced for a very short period (less than 5 minutes) when endocytosis had not yet occurred and the rounding of the cells had just started. After the restoration of standard calcium levels, fluorescent puncta were still taken up into the cell interior but did not relocate to the cell surface (Fig. 10) (Movie 13 available at jcs.biologists.org/supplemental). Instead, small puncta formed at the cell surface starting after 18 minutes; these increased in number and size over time in the continued presence of endocytosed material (compare small and large arrows in Fig. 10). Our observations suggest that clustered desmosomal material that is taken up by endocytosis is not the major source for desmosome reformation. Instead, sufficient desmosomal cadherins appear to be present at the cell surface to facilitate the formation of new desmosomal adhesion sites. Similar small

puncta were also observed in trypsinized cells after replating (not shown). These puncta formed only very slowly but, again, not from particulate precursors in the cytoplasm.

A considerable proportion of desmosomal cadherins is exchanged within 30 minutes

Fluorescence recovery after photobleaching (FRAP) analyses (for a review, see Reits and Neefjes, 2001) were performed to discover whether desmosome stability is reflected by the long residence times of its constituents or is maintained through the continuous exchange of its molecular components. To this end, desmosome-rich contact regions that were located in the middle of continuous MDc-2 monolayers were subjected to photobleaching. As the continuous cell movements made it difficult to determine fluorescence in the areas of interest for extended periods of time, measurements of fluorescence recovery were restricted to the first 30 minutes after photobleaching. In the example shown in Fig. 11A, some fluorescence had re-appeared within 5 minutes following exhaustive bleaching. After 15 minutes, 52% of the original fluorescence had reappeared, rising to 64% by 30 minutes. The percentage of recoverable fluorescence within 30 minutes differed somewhat between cells (60±20%; n=6). The pooled results of six independent experiments are presented in Fig. 11C. The same analyses were also carried out on PDc-13 cells with similar results (Fig. 11B,C). The percentage of recovery after 30 minutes was lower than in MDc-2 cells (36±17%; n=10) but occurred also in an asymptotic manner. Furthermore, in recordings with a setup for high spatial resolution, re-emergence of fluorescence was seen at the same spots that had been labeled prior to bleaching, suggesting that, despite the rapid exchange of subunits, desmosomes remain in loco (Fig. 11D,E,E′).

Discussion

Fluorescent desmosomal cadherin chimeras are well suited for the in vivo detection of desmosomes

The establishment of cell lines containing fluorescent desmosomes that can be monitored in vivo was accomplished via the expression of fluorescent Dsc2a chimeras. These hybrid polypeptides were, for the most part, integrated into desmosomes and, to a lesser extent, in other plasma membrane domains and only occasionally in cytoplasmic vacuolar compartments. We recently observed the same distribution pattern by using a fluorescent Dsg2 fusion protein (R.W. and R.E.L., unpublished). In contrast to the desmosomal cadherins, other major desmosomal proteins are unlikely to confer the same degree of specificity on fluorescent fusion proteins. Plakoglobin is universally present in all adherens junctions (Schmidt et al., 1994; Kowalczyk et al., 1999); it also forms a soluble complex in the cytoplasm (Kapprell et al., 1987) and has been localized in the nucleus when overexpressed (Karnovsky and Klymkowsky, 1995; Simcha et al., 1998). Substantial amounts of all plakophilin isoforms are also expressed in the nucleus in association with particles containing RNA polymerase III (Mertens et al., 1996; Schmidt et al., 1997; Bonné et al., 1999; Mertens et al., 2001) [for fluorescent protein chimeras, see also (Klymkowsky, 1999)], and considerable quantities of desmoplakin are often associated with CKFs, especially in PLC cells (R.W. and R.E.L., unpublished). In addition, the overexpression of desmoplakin has been shown to result frequently in a co-alignment with IFs and their disruption (Stappenbeck et al., 1993). It has been reported that epitope-tagged full-length Dsg can also exert dominant-negative effects when overexpressed, thereby disrupting endogenous desmosome formation, whereas a low expression of these molecules does not appear to interfere with desmosome formation or function (Norvell and Green, 1998). To avoid the dominant-negative phenotype, stable cell lines were generated in this study and subjected to detailed analyses. We found that these lines contained morphologically normal desmosomes that were fully competent to recruit typical CKF bundles. Furthermore, the desmosomes containing fluorescent fusion proteins behaved identically to their counterparts in wild-type cells during mitosis and in the calcium-switch system (cf. Mattey and Garrod, 1986; Baker and Garrod, 1993). Evidence was recently published demonstrating that our choice of Dsc2a was fortunate, as the isoform Dsc1a is not incorporated efficiently into the desmosomes of MDCK cells (Ishii et al., 2001).

Desmosomes are part of a stable network with inherent flexibility and elasticity

A major outcome of our study is that desmosomes are extremely stable, exceeding by far the stability of other cell adhesion structures studied to date (e.g. Jordan et al., 1999; Windoffer et al., 2000). We can rule out the possibility that the high degree of stability reflects specific properties of the cell lines used as the rapid and continuous reorganization of gap junctions has been reported in the same PLC cell line that was used in this study (Windoffer et al., 2000). The stability of desmosomes is quite remarkable in light of the high cell motility seen in the monolayers, which are most notable in MDc-2 cells. The time-space diagrams have revealed that desmosomes are part of an interconnected network reacting in synchrony to cell-shape changes. An important feature of this network is its intrinsic elasticity, which allows the stretching and compression of cell borders without the disruption of the overall arrangement of desmosomal contact sites. This may explain the way in which desmosomal adhesion is maintained during the entire cell cycle and even during mitosis when complete restructuring of the cell takes place. Desmosomes should therefore be considered as one of the major mechanical intercellular integrators that function as stabilizers in a continuously dynamic environment, thereby providing uninterrupted intercellular adhesion, which is especially needed for tissue coherence in mechanically challenged tissues. This function is fulfilled in concert with the IF cytoskeleton, which is organized into a transcellular network by desmosomal adhesion. Consequently, CKF bundles are seen to be tightly associated with desmosomes during interphase and also, albeit to a lesser degree, during mitosis. It appears, however, that different populations of CKFs co-exist: those that are subject to continuous re-structuring (Windoffer and Leube, 1999) and those that are stable throughout the cell cycle and occur in association with desmosomes (this study). These latter CKFs may form, together with the more flexible actin-rich cortex, the linkage between desmosomes, determining their

coordinated motility and maintenance during cell-shape changes (see also Pasdar and Li, 1993). This system of stable structures and interconnecting filaments is reminiscent of the situation in the nucleus where nuclear pore complexes form, together with the nuclear lamina, an immobile and extremely stable network with intrinsic elasticity (Daigle et al., 2001).

Uptake of complete desmosomal plaque assemblies and clustering of desmosomal cadherins contribute to regulation of desmosomal adhesion

Live cell imaging of fluorescent protein chimeras has allowed us to establish precursor/product relationships in single living cells by continuous fluorescence monitoring, thus extending previous observations in fixed cells. We have found that desmosomal adhesion is terminated in LCM by the rapid uptake of desmosomal cadherins into endocytotic structures that have been characterized in the past not only in MDCK cells but also in a number of other epithelial cell lines (Kartenbeck et al., 1982; Mattey and Garrod, 1986; Kartenbeck et al., 1991; Holm et al., 1993). These structures correspond to vesicles that contain complete desmosomal assemblies together with their adhering IFs. Furthermore, we have noted that the uptake of desmosomal halves is dependent on actin filaments, which is in accordance with previous observations (Holm et al., 1993). The uptake has been shown to be independent of clathrin and to reach, initially, a non-lysosomal compartment (Holm et al., 1993), although the desmosomal components are ultimately destined for degradation (Mattey and Garrod, 1986; Burdett, 1993). In support of this, the fluorescence of the endocytosed particles fades over time in our recordings. Our data also strongly suggest that this endocytotic process is irreversible, even at the earliest stages, and therefore cannot serve for the direct re-utilization of desmosomal particles. It remains a possibility, however, that single polypeptide subunits or small aggregates that are below the detection limit of our system are recycled and used for the reformation of desmosomes. In addition to the bulk uptake of desmosomal particles, we have observed that other mechanisms are also operative in LCM and that, depending on cell type and time after plating, endocytosis may be totally prevented (see also Watt et al., 1984; Mattey and Garrod, 1986; Wallis et al., 2000). In particular, we have noted, with the new methods at hand, an increased fusion and fission of desmosomes, and we take this as an indication of their destabilization. We propose that, in these instances, conformational changes of desmosomal cadherins occur and result in the reduction of transcellular adhesiveness, thereby elevating the motility of desmosomal and/or half-desmosomal particles within the plasma membrane. Furthermore, our observation of increased diffuse cell surface staining suggests that some desmosomal cadherins are released from desmosomes, although it may in part be caused by delivery of molecules from biosynthetic or any other, yet unknown compartment. In support, Troyanovsky et al. (Troyanovsky et al., 1999) have reported that the removal of calcium ions results in novel interactions, most notably in the formation of lateral dimers of desmosomal cadherins with E-cadherin. Another indication for desmosomal cadherin dispersion within the plasma membrane in LCM is our observation that new desmosomes are formed soon after the return of cells to SCM, even when endocytosis has just taken place and when endocytotic structures remained in the cell interior (see also Mattey and Garrod, 1986; Garrod et al., 1990).

A different situation is encountered during the formation of new desmosomes. We have not found evidence for the usage of pre-assembled particles as direct precursors for the reformation of desmosomes in the calcium-switch system. In addition, we have observed only a little vesicular desmosomal cadherin fluorescence when cells are cultivated for extended periods in LCM (see also Burdett, 1993). This is in agreement with biochemical analyses demonstrating the increased solubility of desmosomal cadherins in MDCK cells grown in LCM (Penn et al., 1987; Pasdar and Nelson, 1989), indicating that they are not part of large assemblies under these conditions. Therefore, all the analyses carried out so far suggest that desmosomes are formed at the plasma membrane by the maturation of enlarging particles (e.g. Hennings and Holbrook, 1983; Watt et al., 1984; Pasdar and Nelson, 1989), which, however, may rely on cytoplasmic pools of desmosomal plaque components, such as desmoplakins (Duden and Franke, 1988; Pasdar and Nelson, 1988) and plakoglobin (Kapprell et al., 1987). This notion is supported by our observations of desmosome formation that occurs after replenishment of calcium in the calcium-switch system and after trypsinization. Furthermore, other adherens junctions are also formed at the cell surface from diffuse material that accumulates into immobile puncta that grow and mature into fully competent adhesion structures (Adams et al., 1998). In conclusion, the movement of large desmosomal particles is only of functional importance for the bulk removal of split desmosomal halves from the cell surface under certain conditions, whereas small subunits are of relevance in most other instances, determining the assembly of desmosomes at the cell surface and the fine tuning of desmosomal stability. This is in accordance with in vivo observations on other cell adhesion structures (Adams et al., 1998; Jordan et al., 1999; Windoffer et al., 2000; Jordan et al., 2001).

Desmosomal cadherins are subject to continuous turnover

The observed fast exchange of Dsc2a chimeras in SCM was quite unexpected considering the unusual structural stability of desmosomes. Furthermore, preliminary FRAP determinations with a fluorescent Dsg2 fusion protein fully support these data (R.W. and R.E.L., unpublished). In principle, Dsc2a replenishment in the bleached areas may be fuelled from the cytoplasm, from non-desmosomal plasma membrane domains and/or from neighboring desmosomes. Clearly, the cytoplasmic pools cannot account by themselves for the rapid fluorescence recovery given the weak cytoplasmic staining in most cells. Furthermore, the long half-lives of the major pools of desmosomal cadherins in MDCK cells in SCM [20.1±0.4 hours for Dsg1 and 19.6±1.5 hours for Dsc (probably isoforms 2a and 2b) determined by Penn et al. (Penn et al., 1987); more than 24 hours for Dsg1, as determined by Pasdar and Nelson (Pasdar and Nelson, 1989)] also show that a biosynthetic compartment cannot be responsible for the rapid recruitment of desmosomal cadherins. With regard to the last two points, Dsc2a exists in both a desmosomal pool and non-desmosomal pool, which have been visualized by fluorescence microscopy

in the form of puncta and diffuse fluorescence, respectively. Although the majority of polypeptides is clearly concentrated in desmosomes, both pools must be in equilibrium under steady-state conditions. The best explanation for our current results is that rapid exchange takes place between both pools, since we have not found any evidence for vesicular traffic between membrane domains. Furthermore, to account for the recovery of desmosomal fluorescence at distant sites, the non-desmosomal pool must be rapidly diffusible. Given the longevity of desmosomal cadherins (see above), one has to propose that polypeptides are exchanged in and out of desmosomes several times during their lifetime. Exchange rates apparently differ between cell lines and may be influenced by certain, as yet unknown, factors. Currently, it also remains a possibility that desmosomal cadherins with different exchange kinetics co-exist within individual desmosomes. Such an intrinsic heterogeneity could result from differences in packaging density, association with the cytoskeleton, different localization within the plaque and/or protein modification, as has been described for the gap-junction-localized connexins (e.g. Windoffer et al., 2000, Rütz and Hülser, 2001). The attractive implication of the reported FRAP results is the idea that desmosomal stability and durability is combined with a pathway that could serve to adjust desmosomal adhesion rapidly to specific requirements, for example, reversible phosphorylation (Pasdar et al., 1995; van Hengel et al., 1997; Wallis et al., 2000; Gaudry et al., 2001).

We wish to thank Ursula Wilhelm, Antje Leibold, Sabine Thomas and Bernhard Beile for excellent technical assistance. We are grateful to S. Schäfer and W. W. Franke (German Cancer Research Center, Heidelberg) for providing the Dsc2a cDNA and numerous antibodies, to Pavel Strnad (this institute) for help in the preparation of construct C-HK18-ECFP1, and to the group of G. Technau (Department of Genetics, Johannes Gutenberg-University, Mainz) for use of their confocal microscope. This work was supported by grants from the 'Stiftung Rheinland Pfalz für Innovation' and the German Research Council (LE 566/7-1).

References

Adams, C. L., Chen, Y.-T., Smith, S. J. and Nelson, W. J. (1998). Mechanisms of epithelial cell-cell adhesion and cell compaction revealed by high-resolution tracking of E-cadherin-green fluorescent protein. *J. Cell Biol.* **142**, 1105-1119.

Akhtar, N. and Hotchin, N. A. (2001). RAC1 regulates adherens junctions through endocytosis of E-cadherin. *Mol. Biol. Cell* **12**, 847-862.

Bader, B. L., Magin, T. M., Freudenmann, M., Stumpp, S. and Franke, W. W. (1991). Intermediate filaments formed de novo from tail-less cytokeratins in the cytoplasm and in the nucleus. *J. Cell Biol.* **115**, 1293-1307.

Baker, J. and Garrod, D. (1993). Epithelial cells retain junctions during mitosis. *J. Cell Sci.* **104**, 415-425.

Bonné, S., van Hengel, J., Nollet, F., Kools, P. and van Roy, F. (1999). Plakophilin-3, a novel armadillo-like protein present in nuclei and desmosomes of epithelial cells. *J. Cell Sci.* **112**, 2265-2276.

Burdett, I. D. J. (1993). Internalisation of desmosomes and their entry into the endocytic pathway via late endosomes in MDCK cells. Possible mechanisms for the modulation of cell adhesion by desmosomes during development. *J. Cell Sci.* **106**, 1115-1130.

Burdett, I. D. J. (1998). Aspects of the structure and assembly of desmosomes. *Micron* **29**, 309-328.

Daigle, N., Beaudouin, J., Hartnell, L., Imreh, G., Hallberg, E., Lippincott-Schwartz, J. and Ellenberg, J. (2001). Nuclear pore complexes form immobile networks and have a very low turnover in live cells. *J. Cell Biol.* **154**, 71-84.

Demlehner, M. P., Schäfer, S., Grund, C. and Franke, W. W. (1995). Continual assembly of half-desmosomal structures in the absence of cell contacts and their frustrated endocytosis: a coordinated Sisyphus cycle. *J. Cell Biol.* **131**, 745-760.

Duden, R. and Franke, W. W. (1988). Organization of desmosomal plaque proteins in cells growing at low calcium concentrations. *J. Cell Biol.* **107**, 1049-1063.

Gaudry, C. A., Palka, H. L., Dusek, R. L., Huen, A. C., Khandekar, M. J., Hudson, L. G. and Green, K. J. (2001). Tyrosine-phosphorylated plakoglobin is associated with desmogleins but not desmoplakin after epidermal growth factor receptor activation. *J. Biol. Chem.* **276**, 24871-24880.

Garrod, D. R., Parrish, E. P., Mattey, D. L., Marston, J. E., Measures, H. R. and Vilela, M. J. (1990). Desmosomes. In *Intercellular Junctions and Cell Adhesion in Epithelial Cells* (eds G. M. Edelman, B. A. Cunningham and J.-P. Thiery), pp. 315-339. Chichester: John Wiley.

Hennings, H. and Holbrook, K. A. (1983). Calcium regulation of cell-cell contact and differentiation of epidermal cells in culture. *Exp. Cell Res.* **143**, 127-142.

Holm, P. K., Hansen, S. H., Sandvig, K. and van Deurs, B. (1993). Endocytosis of desmosomal plaques depends on intact actin filaments and leads to a nondegradative compartment. *Eur. J. Cell Biol.* **62**, 362-371.

Holm, I., Mikhailov, A., Jillson, T. and Rose, B. (1999). Dynamics of gap junctions observed in living cells with connexin43-GFP chimeric protein. *Eur. J. Cell Biol.* **78**, 856-866.

Ishii, K., Norvell, S. M., Bannon, L. J., Amargo, E. V., Pascoe, L. T. and Green, K. J. (2001). Assembly of desmosomal cadherins into desmosomes is isoform dependent. *J. Invest. Dermatol.* **117**, 26-35.

Jordan, K., Solan, J. L., Dominguez, M., Sia, M., Hand, A., Lampe, P. D. and Laird, D. W. (1999). Trafficking, assembly, and function of a connexin43-green fluorescent protein chimera in live mammalian cells. *Mol. Biol. Cell* **10**, 2033-2050.

Jordan, K., Chodock, R., Hand, A. R. and Laird, D. W. (2001). The origin of annular junctions: a mechanism of gap junction internalization. *J. Cell Sci.* **114**, 763-773.

Kapprell, H.-P., Cowin, P. and Franke, W. W. (1987). Biochemical characterization of the soluble form of the junctional plaque protein, plakoglobin, from different cell types. *Eur. J. Cell Biol.* **166**, 505-517.

Karnovsky, A. and Klymkowsky, M. W. (1995). Over-expression of plakoglobin leads to dorsalization and axis duplication in *Xenopus*. *Proc. Natl. Acad. Sci. USA* **92**, 4522-4526.

Kartenbeck, J., Schmid, E., Franke, W. W. and Geiger, B. (1982). Different modes of internalization of proteins associated with adhaerens junctions and desmosomes: experimental separation of lateral contacts induces endocytosis of desmosomal plaque material. *EMBO J.* **1**, 725-732.

Kartenbeck, J., Schmelz, M., Franke, W. W. and Geiger, B. (1991). Endocytosis of junctional cadherins in bovine kidney epithelial (MDBK) cells cultured in low Ca^{2+} ion medium. *J. Cell Biol.* **113**, 881-892.

Klymkowsky, M. W. (1999). Plakophilin, armadillo repeats, and nuclear localization. *Microsc. Res. Tech.* **45**, 43-54.

Kowalczyk, A. P., Palka, H. L., Luu, H. H., Nilles, L. A., Anderson, J. E., Wheelock, M. J. and Green, K. J. (1994). Posttranslational regulation of plakoglobin expression. Influence of the desmosomal cadherins on plakoglobin metabolic stability. *J. Biol. Chem.* **49**, 31214-31223.

Kowalczyk, A. P., Bornslaeger, E. A., Norvell, S. M., Palka, H. L. and Green, K. J. (1999). Desmosomes: intercellular adhesive junctions specialized for attachment of intermediate filaments. *Int. Rev. Cytol.* **185**, 237-302.

Le, T. L., Yap, A. S. and Stow, J. L. (1999). Recycling of E-cadherin: a potential mechanism for regulating cadherin dynamics. *J. Cell Biol.* **146**, 219-232.

Leube, R. E. (1995). The topogenic fate of the polytopic transmembrane proteins, synaptophysin and connexin, is determined by their membrane-spanning domains. *J. Cell Sci.* **108**, 883-894.

Mattey, D. L. and Garrod, D. R. (1986). Splitting and internalization of the desmosomes of cultured kidney epithelial cells by reduction in calcium concentration. *J. Cell Sci.* **85**, 113-124.

Mertens, C., Kuhn, C. and Franke, W. W. (1996). Plakophilins 2a and 2b: constitutive proteins of dual location in the karyoplasm and the desmosomal plaque. *J. Cell Biol.* **135**, 1009-1025.

Mertens, C., Hofmann, I., Whang, Z., Teichmann, M., Chong, S. S., Schnôlzer, M. and Franke, W. W. (2001). Nuclear particles containing RNA polymerase III complexes associated with the junctional plaque protein plakophilin 2. *Proc. Natl. Acad. Sci. USA* **98**, 7795-7800.

Moll, R. and Moll, I. (1998). Epidermal adhesion molecules and basement membrane components as target structures of autoimmunity. *Virch. Arch.* **432**, 487-504.

North, A. J., Bardsley, W. G., Hyam, J., Bornslaeger, E. A., Cordingley, H. C., Trinnaman, B., Hatzfeld, M., Green, K. J., Magee, A. I. and Garrod, D. R. (1999). Molecular map of the desmosomal plaque. *J. Cell Sci.* **112**, 4325-4336.

Norvell, S. M. and Green, K. J. (1998). Contributions of extracellular and intracellular domains of full length and chimeric cadherin molecules to junction assembly in epithelial cells. *J. Cell Sci.* **111**, 1305-1318.

Oda, H. and Tsukita, S. (1999). Dynamic features of adherens junctions during Drosophila embryonic epithelial morphogenesis revealed by a Dα-catenin-GFP fusion protein. *Dev. Genes Evol.* **209**, 218-225.

Parker, A. E., Wheeler, G. N., Arnemann, J., Pidsley, S. C., Ataliotis, P., Thomas, C. L., Rees, D. A., Magee, A. I. and Buxton, R. S. (1991). Desmosomal glycoproteins II and III. Cadherin-like junctional molecules generated by alternative splicing. *J. Biol. Chem.* **266**, 10438-10445.

Pasdar, M. and Li, Z. (1993). Disorganization of microfilaments and intermediate filaments interferes with the assembly and stability of demosomes in MDCK cells. *Cell Motil. Cytoskeleton* **26**, 163-180.

Pasdar, M. and Nelson, W. J. (1988). Kinetics of desmosome assembly in Madin-Darby canine kidney epithelial cells: temporal and spatial regulation of desmoplakin organization and stabilization upon cell-cell contact. I. Morphological analysis. *J. Cell Biol.* **106**, 687-695.

Pasdar, M. and Nelson, W. J. (1989). Regulation of desmosome assembly in epithelial cells: kinetics of synthesis, transport, and stabilization of desmoglein I, a major protein of the membrane core domain. *J. Cell Biol.* **109**, 163-177.

Pasdar, M., Li, Z. and Chan, H. (1995). Desmosome assembly and disassembly are regulated by reversible protein phosphorylation in cultured epithelial cells. *Cell Motil. Cytoskeleton* **30**, 108-121.

Penn, E. J., Burdett, I. D. J., Hobson, C., Magee, A. I. and Rees, D. A. (1987). Structure and assembly of desmosome junctions: biosynthesis and turnover of the major desmosome components of Madin-Darby kidney cells in low calcium medium. *J. Cell Biol.* **105**, 2327-2334.

Reits, E. A. J. and Neefjes, J. J. (2001). From fixed to FRAP: measuring protein mobility and activity in living cells. *Nat. Cell Biol.* **3**, E145-E147.

Rütz, M. L. and Hülser, D. F. (2001). Supramolecular dynamics of gap junctions. *Eur. J. Cell Biol.* **80**, 20-30.

Schäfer, S., Koch, P. J. and Franke, W. W. (1994). Identification of the ubiquitous human desmoglein, Dsg2, and the expression catalogue of the desmoglein subfamily of desmosomal cadherins. *Exp. Cell Res.* **211**, 391-399.

Schmidt, A., Heid, H. W., Schäfer, S., Nuber, U. A., Zimbelmann, R., Franke, W. W. (1994). Desmosomes and cytoskeletal architecture in epithelial differentiation: cell type-specific plaque components and intermediate filament anchorage. *Eur. J. Cell Biol.* **65**, 229-245.

Schmidt, A., Langbein, L., Rode, M., Prätzel, S., Zimbelmann, R. and Franke, W. W. (1997). Plakophilins 1a and 1b: widespread nuclear proteins recruited in specific eptihelial cells as desmosomal plaque components. *Cell Tissue Res.* **290**, 481-499.

Simcha, I., Shtutman, M., Salomon, D., Zhurinsky, J., Sadot, E., Geiger, B. and Ben-Ze'ev, A. (1998). Differential nuclear translocation and transactivation potential of β-catenin and plakoglobin. *J. Cell Biol.* **141**, 1433-1448.

Stappenbeck, T. S., Bornslaeger, E. A., Corcoran, C. M., Luu, H. H., Virata, M. L. and Green, K. J. (1993). Functional analysis of desmoplakin domains: specification of the interaction with keratin versus vimentin intermediate filament networks. *J. Cell Biol.* **123**, 691-705.

Strnad, P., Windoffer, R. and Leube, R. E. (2001). In vivo detection of cytokeratin filament network breakdown in cells treated with the phosphatase inhibitor okadaic acid. Cell Tissue Res. **306**, 277-293.

Troyanovsky, S. M. and Leube, R. E. (1998). Molecular dissection of desmosomal assembly and intermediate filament anchorage. In *Intermediate Filaments* (ed. H. Herrmann and J. R. Harris), pp. 263-289. New York: Plenum Press.

Troyanovsky, R. B., Klingelhöfer, J. and Troyanovsky, S. (1999). Removal of calcium ions triggers a novel type of intercadherin interaction. *J. Cell Sci.* **112**, 4379-4387.

Udey, M. C. and Stanley, J. R. (1999). Pemphigus – Diseases of antidesmosomal autoimmunity. *JAMA* **282**, 572-576.

van Hengel, J., Gohon, L., Bruyneel, E., Vermeulen, S., Cornelissen, M., Mareel, M. and van Roy, F. (1997). Protein kinase C activation upregulates intercellular adhesion of β-catenin-negative human colon cancer cell variants via induction of desmosomes. *J. Cell Biol.* **137**, 1103-1116.

Wallis, S., Lloyd, S., Wise, I., Ireland, G., Fleming, T. P. and Garrod, D. (2000). The α isoform of protein kinase C is involved in signaling the response of desmosomes to wounding in cultured epithelial cells. *Mol. Biol. Cell* **11**, 1077-1092.

Watt, F. M., Mattey, D. L. and Garrod, D. R. (1984). Calcium-induced reorganization of desmosomal components in cultured human keratinocytes. *J. Cell Biol.* **99**, 2211-2215

Windoffer, R. and Leube, R. E. (1999). Detection of cytokeratin dynamics by time-lapse fluorescence microscopy in living cells. *J. Cell Sci.* **112**, 4521-4534.

Windoffer, R. and Leube, R. E. (2001). De novo formation of cytokeratin filament networks originates from the cell cortex in A-431 cells. *Cell Motil. Cytoskeleton* **50**, 33-44.

Windoffer, R., Beile, B., Leibold, A., Thomas, S., Wilhelm, U. and Leube, R. E. (2000). Visualization of gap junction mobility in living cells. *Cell Tissue Res.* **299**, 347-362.